

Study on the Pulmonary Delivery System of Apigenin-Loaded Albumin Nanocarriers with Antioxidant Activity

Zsófia Edit Pápay, PharmD,¹ Annamária Kósa, PhD,² Be'la Bo'ddi, PhD,² Zahra Merchant, MRes,³ Imran Y Saleem, PhD,⁴ Mohammed Gulrez Zariwala, PhD,⁵ Imre Klebovich, PhD,¹ Satyanarayana Somavarapu, PhD,³ and István Antal, PhD¹

Background: Respiratory diseases are mainly derived from acute and chronic inflammation of the alveoli and bronchi. The pathophysiological mechanisms of pulmonary inflammation mainly arise from oxidative damage that could ultimately lead to acute lung injury. Apigenin (Api) is a natural polyphenol with prominent antioxidant and anti-inflammatory properties in the lung. Inhalable formulations that consist of nanoparticles (NPs) have several advantages over other administration routes, and therefore, this study investigated the application of apigenin-loaded bovine serum albumin nanoparticles (BSA-Api-NPs) for pulmonary delivery.

Methods: Dry powder formulations of BSA-Api-NPs were prepared by spray drying and characterized by laser diffraction particle sizing, scanning electron microscopy, differential scanning calorimetry, and powder X-ray diffraction. The influence of dispersibility enhancers (lactose monohydrate and L-leucine) on the *in vitro* aerosol deposition using a next-generation impactor was investigated in comparison to excipient-free formulation. The dissolution of Api was determined in simulated lung fluid by using the Franz cell apparatus. The antioxidant activity was determined by 2,2-diphenyl-1-picrylhydrazyl (DPPH·) free radical scavenging assay.

Results: The encapsulation efficiency and the drug loading were measured to be $82.61\% \pm 4.56\%$ and $7.51\% \pm 0.415\%$. The optimized spray drying conditions were suitable to produce particles with low residual moisture content. The spray-dried BSA-Api-NPs possessed good aerodynamic properties due to small and wrinkled particles with low mass median aerodynamic diameter, high emitted dose, and fine particle fraction. The aerodynamic properties were enhanced by leucine and decreased by lactose, however, the dissolution was reversely affected. The DPPH· assay confirmed that the antioxidant activity of encapsulated Api was preserved.

Conclusion: This study provides evidence to support that albumin nanoparticles are suitable carriers of Api and the use of traditional or novel excipients should be taken into consideration. The developed BSA-Api-NPs are a novel delivery system against lung injury with potential antioxidant activity.

Keywords: aerosol distribution, inhaled therapy, modeling, flavonoid

Introduction

RESPIRATORY DISEASES ARE THOUGHT TO BE mainly derived from acute and chronic inflammation of the alveoli and bronchi. The pathophysiological mechanisms of pulmonary inflammation arise from several factors, including

oxidative damage due to cytotoxic mediators that may ultimately lead to acute lung injury (ALI), acute respiratory distress syndrome, and cancer.⁽¹⁾ A growing body of scientific data suggests that natural occurring compounds possess

¹Department of Pharmaceutics, Semmelweis University, Budapest, Hungary.

²Department of Plant Anatomy, Institute of Biology, Eötvös Loránd University, Budapest, Hungary.

³Department of Pharmaceutics, UCL School of Pharmacy, London, United Kingdom.

⁴Formulation and Drug Delivery Research, School of Pharmacy and Biomolecular Sciences, Liverpool John Moores University, Liverpool, United Kingdom.

⁵Department of Biomedical Science, Faculty of Science and Technology, University of Westminster, London, United Kingdom.

preventive and therapeutic properties with inherent low toxicity.⁽²⁾ Among phytochemicals, apigenin (Api; Fig. 1) is a promising candidate as a therapeutic agent, mainly due to its antioxidant and anti-inflammatory properties.⁽³⁻⁶⁾ It has been demonstrated that Api has protective effects against bleomycin-induced lung fibrosis in rats, which is associated with its antioxidant and anti-inflammatory capacities.⁽⁷⁾

Another study provided evidence that Api was able to decrease oxidative stress and inflammation on paraquat-induced ALI in mice⁽⁸⁾ and reduced the pathological alterations of pulmonary tissue in acute pancreatitis-associated ALI, therefore suggesting protection in the lung.⁽⁹⁾ Furthermore, Api has an anti-inflammatory effect owing to significant inhibition of proinflammatory cytokines, activator protein (AP-1), and cyclooxygenase-2 (COX-2) in human pulmonary epithelial cells⁽¹⁰⁾ and in mice as well.⁽¹¹⁾ However, Api has low water solubility (2.16 g/mL at pH 7.5), and therefore, it was recently classified as Biopharmaceutical Classification System (BCS) II drug.⁽¹²⁾

Encapsulation and delivery of phytoconstituents with health effects have attracted much attention in recent years. Developing a suitable carrier system is essential to improve the overall activity and reduce the possible toxicity of these agents.⁽¹³⁾ Among the potential carrier systems, serum albumin nanoparticles have notable advantages, including biodegradability, nonantigenicity, and cell-targeting ability.^(14,15) Moreover, albumin provides exceptional ligand binding capacity for various drugs owing to three homologous domains with two separate helical subdomains.⁽¹⁶⁾ Studies reported the successful incorporation of flavonoids into albumin nanoparticles that can improve their stability⁽¹⁷⁾ and antitumor activity.⁽¹⁸⁾

Pulmonary delivery of pharmacologically active ingredients is extensively studied due to prominent advantages over other delivery routes of administration.⁽¹⁹⁾ The lungs have a large surface area, limited enzymatic activity, and high permeability; therefore, drugs can be delivered either locally for the treatment of respiratory diseases or systematically to, for example, avoid first-pass metabolism.⁽²⁰⁾ Dry powder inhaler products offer precise and reproducible delivery of fine drug particle fraction to the deep lung and recent studies have proved that these are more cost-effective than other products.⁽²¹⁾ This noninvasive delivery route could be suitable for poorly water soluble drugs in nanoparticles with increased solubility.⁽²²⁾

It is also well recognized that nanoparticles have benefits over other carriers in the micron scale such as controlled drug release, avoiding mucociliary clearance, and improved

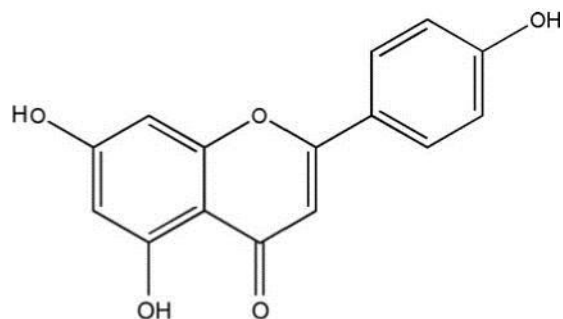


FIG. 1. Molecular structure of apigenin. deposition.^(23,24) Albumin is naturally present in the body, as well as in the lung epithelium,⁽²⁴⁾ moreover, the body can

absorb proteins into the bloodstream by transcytosis, which occurs deep in the lung and allows drug molecules to pass through cell membrane.⁽²⁵⁾ Therefore, the presence of bovine serum albumin (BSA) in the nanoparticle system increases membrane permeability and may facilitate epithelial cell uptake and translocation through the alveolar-capillary barrier of the lung.⁽²⁶⁾ It was proved that albumin nanoparticles have high biocompatibility in a wide dose range and remained longer in the lungs with low systemic exposure.⁽²⁴⁾ Thus, encapsulation of apigenin into albumin nanoparticles would enhance its solubility and distribution in the lung.

However, the formulation of dry powders with optimal aerodynamic properties for pulmonary drug delivery is challenging. Spray drying is a technique for manufacturing respirable dry powders in one step. During the process, the liquid phase is atomized into droplets that dry rapidly in the drying chamber due to compressed air. The process conditions such as heat, flow rate, aspiration rate, and pump rate also determine the quality of the product. The thermal degradation caused by overheating can be avoided by the rapid evaporation of the solvent.⁽²⁷⁾ Hence, it is suitable for drying colloidal systems resulting in uniform particle morphology.

Nanoparticle delivery systems targeted to the lungs offer several advantages such as sustained release, increased local drug concentration, and targeted site of action.⁽²⁸⁾ Moreover, improved drug solubility, uniform dose distribution, and fewer side effects can be achieved, compared to conventional dry powders. In general, respirable nanoparticles are embedded in microparticles in aerodynamic size range.⁽²⁶⁾

The aim of this work was to develop a novel dry powder formulation against ALI caused by oxidative stress. The prepared albumin nanoparticles were characterized in terms of size, zeta potential, and drug loading; in addition, the fluorescence properties were investigated. Following this, the nanoparticles were spray dried with two types of excipients, namely a traditional lactose monohydrate and a novel amino acid, L-leucine. *In vitro* aerosol deposition patterns were determined in comparison to an excipient-free formulation using a next-generation impactor (NGI), and a dissolution test was performed in simulated lung fluid by using Franz cell apparatus. Laser diffraction particle sizing, morphology, and residual moisture content were measured along with the antioxidant activity.

Materials and Methods

Apigenin (Api) was purchased from (purity >99%) Hangzhou DayangChem Co., Ltd. (China). BSA powder (purity +98%), L-leucine, analytical-grade chloroform, acetonitrile, and trifluoroacetic acid (TFA) were obtained from Sigma Aldrich Ltd. (Dorset, United Kingdom). Lactohale[®] LH 230 was supplied by Friesland Foods Domo (Amersfoort, The Netherlands). 2,2-Diphenyl-1-picrylhydrazyl (DPPH[•]) free radical was purchased from Sigma Aldrich (Darmstadt, Germany). For the solubility and drug release study, PBS buffer was purchased (Sigma Aldrich Ltd.) and modified simulated lung fluid with 0.02% (w/v) (mSLF) was prepared. All of the materials for the mSLF were purchased from Sigma Aldrich Ltd.

Preparation of BSA-NPs

BSA nanoparticles were prepared using a nanoparticle albumin-bound technology with minor modifications.⁽²⁹⁾ Briefly, 1000mg of BSA was dissolved in 50 mL of distilled water saturated with chloroform. Separately, 100mg of Api was dissolved in 3 mL of chloroform saturated with water and ultrasonicated for 10 minutes. These two solutions were mixed and ultrasonicated for 20 minutes with a probe-type sonicator (MSE Soniprep 150 Ultrasonic Processor; MSE Ltd., London, United Kingdom) on ice. After homogenization, the chloroform was evaporated by rotary evaporator (Rotavapor® R-10; BÜCHI Labortechnik AG, Flawil, Switzerland) at 25 °C for 15 minutes. The obtained nanoparticles were filtered through filter paper (0.45 µm; Fisher Scientific Ltd., Loughborough, United Kingdom) and further spray dried.

Characterization of BSA-Api-NPs

Particle size and zeta potential analysis. The average particle size and polydispersity index (PDI) were determined by dynamic light scattering using Zetasizer Nano ZS instrument (Malvern Instruments Ltd., Worcestershire, United Kingdom). Zeta potential of the particles was quantified with laser doppler velocimetry using the same instrument. All measurements were performed in triplicate ($n = 3$) at 25 °C and presented as mean \pm standard deviation.

Determination of drug loading and encapsulation efficiency. To determine the amount of Api, 1 mL sample from the BSA-Api formulation was withdrawn and the apigenin content was determined in mg/mL by adding 5 mL of dimethyl sulfoxide and methanol (DMSO:MeOH, 50:50% v/v) and sonicated for 10 minutes. The exact concentrations were determined after filtration (0.22 µm) by HPLC 1260 (Agilent Technologies, Inc., Santa Clara, CA) using the reverse-phase C₁₈ column (Phenomenex®, 250 × 4.6 mm, 4 µm) as the stationary phase. The temperature was set to 25 °C. The mobile phase consisted of 40% acetonitrile and 60% water containing 0.1% (v/v) TFA. The system was run isocratically at the flow rate of 1.2 mL/min and the Api was detected at 340nm ($t_R=8.3$). The injection volume was set to 10 L. A calibration curve was conducted by diluting stock solution (0.1 mg/mL) with R² value of 0.999.

The drug loading efficiency (DL, %) and encapsulation efficiency (EE, %) were calculated according to the equations (Eqs. 1 and 2), comparing the encapsulated Api content (mg/mL, $W_{\text{encapsulated}}$) to total nanoparticle system, which means the weighted amount of BSA and Api together (mg/mL, W_{total}) and the amount of Api (mg/mL, $W_{\text{theoretical}}$) used in the formulations.

$$\frac{W_{\text{encapsulated}}}{W_{\text{total}}} \times 100 \quad (\text{Eq 1})$$

$$EE (\%) = \frac{W_{\text{encapsulated}}}{W_{\text{theoretical}}} \times 100 \quad (\text{Eq 2})$$

Fluorescence spectroscopy. The fluorescence emission spectra of BSA and BSA-Api-NPs were measured with the Jobin Yvon-Horiba Fluoromax-3 (Paris, France) spectroflu-

orometer. The samples that contained the nanoparticles were diluted 10 times, and the fluorescence emission spectra were recorded between 300 and 450nm at 25 °C where the excitation wavelength was set to 285 nm. The data collection frequency was 0.5 nm and the integration time was 0.2 second. The excitation slit was set at a bandpass width of 2 nm and the emission slit at 5 nm. Each spectrum was recorded three times and the mean values were calculated automatically. The SPSERV V3.14 software (© Csaba Bagyinka, Institute of Biophysics, Biological Research Center of the Hungarian Academy of Sciences, Szeged, Hungary) was used for baseline correction, for five-point linear smoothing, and for the correction to the wavelength-dependent sensitivity changes of the spectrofluorometer. The subtraction of the Raman band at 390 nm was performed.

To obtain the three-dimensional (3D) projections and contour maps of fluorescence spectra of the samples, the fluorescence emission was recorded from 265 to 450 nm using different excitation wavelengths from 250 to 310 nm with 10nm steps with the same instrument mentioned above. All emission scan ranges were set to start at least 15 nm away from the corresponding excitation wavelengths. Other settings were similar as described above. Each spectrum was recorded three times and the mean values were calculated automatically. The 3D fluorescence spectra were visualized with the software SURFER Version 10 (Golden Software, Inc., Golden, CO). Spectra were combined together into a 3D surface data set with axes of excitation and emission wavelengths and fluorescence intensity. Data were also converted into two-dimensional contour maps.

Spray drying of BSA-Api-NPs

Spray drying of the BSA-Api formulations without excipient and in the presence of lactose monohydrate (50%, w/w) and L-leucine (9%, w/w) was carried out in a BUCHI

290 Mini Spray Dryer (BUCHI Labortechnik AG, Flawil, Switzerland). The concentration of the excipients was with respect to the mass of the nanoparticles before spray drying. The following operating conditions were used based on pilot experiments: inlet temperature 120 °C, approximate outlet temperature 65 °C–70 °C, the drying airflow 600 L/h, aspiration rate 100% (35 m³/h), the nozzle diameter was 0.1mm, and the liquid feed rate was set to 5 mL/min. Each preparation was carried out in triplicate. Following spray drying, the powders were collected from the lower part of the cyclone and the collecting vessel, stored in tightly sealed glass vials under vacuum at room temperature.

Characterization of spray-dried BSA-Api-NPs

Determination of residual moisture. The moisture content of the spray-dried powders was measured by using Karl Fischer titration (Metrohm 758 KFD Titirino; Metrohm AG, Lichtenstein, Switzerland). For that purpose, –100 mg of the product was analyzed and the instrument was previously calibrated with 10 L distilled water. The evaluation was conducted in triplicate and the standard deviation calculated.

Fourier transform infrared spectroscopy. Fourier transform infrared spectroscopy (FT-IR) spectra of BSA-Api

spray-dried samples were evaluated using a PerkinElmer Spectrum 100 FT-IR spectrometer equipped with Universal ATR (attenuated total reflectance) accessory (PerkinElmer, Inc., Waltham, MA). Approximately 2mg of the solid samples was placed between the plate and the probe. The spectra were recorded with three scans, in the frequency range between 4000 and 600 cm^{-1} and with a resolution of 4 cm^{-1} at room temperature. The data were analyzed using the PerkinElmer Spectrum Express software.

X-ray powder diffraction. X-ray powder diffraction (XRPD) diffractograms were obtained using an X-ray diffractometer (MiniFlex600; Rigaku Corporation, Tokyo, Japan). The analyses were performed at room temperature and the samples were scanned from 2° to 40° 2 θ using a scanning speed of 2°/min with a step size of 0.05°.

Differential scanning calorimetry analysis. The spray-dried formulations were characterized by differential scanning calorimetry (DSC) (DSC Q2000 module; TA Instruments, New Castle, United Kingdom), which was calibrated using indium. Samples (3–5 mg) were weighed accurately and analyzed in sealed and pierced aluminum hermetic pans (TA Instruments). The pans were equilibrated at 25°C and then heated at a rate of 10°C/min in a range of 50°C–400°C.

Aerosol particle size analysis and redispersibility in water. The particle size analysis was conducted by using a Sympatec HELOS laser diffractometer (Sympatec GmbH System-Partikel-Technik, Clausthal-Zellerfeld, Germany). The powders were dispersed by compressed air (4–5 bar) into the measuring zone of the laser beam. The optical lens (0.45–87.5 μm size range) focused onto the detector to collect the diffracted light for calculation of size distribution. The values of 10th (D_{10}), 50th (D_{50}), and 90th (D_{90}) of the cumulative particle size distribution are generated. Samples were measured in triplicate.

The particle size was also determined after spray drying. Five milligrams of dry powder of each formulation could be easily redispersed in 5 mL distilled water and the particle size was determined without any further dilution by the abovementioned Zetasizer Nano ZS instrument (Malvern Instruments Ltd., Worcestershire, United Kingdom).

Solubility and drug release studies of BSA-Api formulations. The solubility of BSA-Api formulations was determined in PBS buffer (pH 7.4) and in mSLF (pH 7.4), which contained 0.02% (w/v) DPPC, prepared according to Son and McConville.⁽³⁰⁾ Fifty milligrams of samples of spray-dried powders was added to 100 mL solvent and shaken (150 rpm) for 2 hours at 37°C. At predetermined time points, 1 mL of samples was taken from each dissolution medium and replaced with the same volume of fresh medium. All of the samples were diluted with 1 mL methanol and filtered with Amicon® Ultra Centrifugal filters (30K; Merck Millipore, Merck KGaA, Germany) before the injection and the amount of apigenin was determined by the HPLC-UV method.

The *in vitro* drug release study of the three formulations was conducted with the Franz cell apparatus. The mSLF was used as dissolution media and a 0.45 μm cellulose acetate membrane filter (Sartorius AG, Gottingen, Germany) was applied.

Briefly, an accurately weighed amount (10 mg) of spray-

dried nanoparticles of each formulations were scattered onto the membrane, which was previously wetted with the dissolution media for 1 hour. One milliliter of samples was withdrawn at various time intervals for 5 hours and replaced with fresh dissolution medium. After the measurement, membrane was rinsed with 2 mL of MeOH and the drug content of the possibly remained powders was determined. The sample preparation and the measurement were the same as mentioned above. The cumulative amount of apigenin release over the time was plotted for each formulation. All measurements were performed in triplicate.

Aerosol delivery of BSA-Api formulations. *In vitro* aerodynamic performance of BSA-Api formulations was assessed using the NGI (Copley Scientific Ltd., Nottingham, United Kingdom), connected sequentially to a low-capacity pump via the critical flow controller (Model LCP5; Copley Scientific Ltd.). During the measurement, the pump was operated at an air flow rate of 60 L/min for 4 seconds. The 3 × 10mg powder aliquots from each formulation were loaded manually into gelatin capsules (size 3) and placed into the inhaler device (Cyclohaler®; Pharmachemie, London, United Kingdom), which was connected to the NGI via an airtight rubber adaptor and a stainless steel United States Pharmacopeia (USP) throat. The NGI stages were assembled with an induction port and a preseparator, and a filter was placed in the final stage.

Before the impaction, the collection plates were uniformly coated with 1 mL of 1% silicone oil in N-hexane solution and allowed to dry, leaving a thin film of silicone oil on the plate surface to prevent the re-entrainment of the particles and the preseparator was filled with 15 mL DMSO:MeOH (50:50%, v/v) mixture. After the deposition of the powders in the NGI, the amount of each formulation was cumulatively collected onto silicone-coated plates for each of the stages. The inhaler, mouthpiece, induction port, preseparator, and the collection plates were rinsed with DMSO:MeOH (50:50%, v/v) mixture, collected in volumetric flasks (10 or 25 mL), and made up to volume. The samples were determined by using the HPLC method as described previously.

To characterize the aerosol performance, the following parameters were calculated based on the drug mass of each fraction: emitted dose (ED, %): the percentage of the entire dose depositing from the mouthpiece of the inhaler device and recovered dose (RD, %): the total recovered drug mass. The fine particle fraction (FPF, <4.46 μm) is defined as the percentage of the ED, deposited from Stage 2–7 and the micro-orifice collector. The mass median aerodynamic diameter (MMAD) and geometric standard deviation (GSD) were calculated from the inverse of the standard normal cumulative mass distribution against the natural logarithm of the effective cutoff diameter of the respective stages. All measurements were carried out in triplicate.

Particle morphology. Morphology of Api powder and spray-died nanoparticles was examined using scanning electron microscopy (SEM) analysis. The dry powder of the formulations was placed on the sample holder using a double adhesive tape, and gold coating (–20 nm thickness) was applied. Examinations were performed by the FEI

Inspect™ S50 (Hillsboro, OR) scanning electron microscope at 20.00 kV accelerating voltage. Original magnifications were 8000 \times , 10,000 \times , and 20,000 \times with accuracy of $\pm 2\%$.

Antioxidant activity

The antioxidant activities of the prepared spray-dried formulations were compared to the pure Api to investigate the effectiveness of the formulation. The free radical scavenging activity was measured by using DPPH_c method as described previously,⁽³¹⁾ with slight modifications. Methanolic stock solution of 0.1 mM DPPH_c reagent was freshly prepared and protected from light. Standard curve was plotted between the DPPH_c concentration (0.01–0.1 mM) and absorbance, the linear relationship was calculated graphically. One milliliter of MeOH was added to the BSA-Api-NPs and the concentration of Api was the same in each sample for comparability. Thereafter, 2 mL of 0.06mM DPPH_c reagent was added to the samples, vortex mixed for 10 seconds, and protected from light.

The absorbance at 517 nm was determined with a spectrophotometer (UV-Vis spectrophotometer, Metertech SP-8001; Metertech, Inc., Taipei, Taiwan) every 15 minutes until the steady state (when no further discoloration could be observed). The addition of samples resulted in a decrease in the absorbance of DPPH_c due to the scavenging activity of Api. The exact concentration of the free radical was calculated using the standard curve. To calculate the inhibition of the free radical DPPH_c, the following equation (Eq. 3) was used:

$$I(\%) = \frac{A_0 - A_s}{A_0} \times 100 \quad (\text{Eq. 3})$$

Where I (%) is the inhibition in percent, A₀ is the absorbance of the DPPH_c solution, and A_s is the absorbance of the sample. All measurements were carried out triplicate and the data are expressed as the mean value \pm standard deviation.

Results and Discussion

Characterization of BSA-Api-NPs

Size, zeta potential, and drug content. Albumin is a natural protein that has been widely used as a macromolecular carrier for many drugs with low water solubility. Several techniques are available to prepare albumin nanoparticles, including desolvation (coacervation), nab (nanoparticle albumin bound) technology, and self-assembly.⁽¹⁴⁾ In this study, the BSA-Api-NPs were prepared by using modified nab technology with ultrasonication. The achieved mean particle size of three samples was 376 ± 7.824 nm with a PDI of 0.285 ± 0.01 . The size of albumin NPs less than 500nm could localize effectively in the lung. The PDI value indicated narrow particle size distribution and the uniformity of the nanoparticles. The zeta potential was -19.20 ± 0.818 mV. The higher the zeta potential, the more stable the formulation is, less aggregation occurs.⁽³²⁾

The EE was determined to be $82.61\% \pm 4.56\%$ and the DL was $7.51\% \pm 0.415\%$. Therefore, these results confirmed the high encapsulation efficiency of apigenin by BSA-NPs and that it can be an attractive tool in encapsulation of flavonoids for delivery. Similar data were found in the literature when encapsulating flavonoids into albumin nanoparticles.

Human serum albumin (HSA)-bound curcumin nano-

particles resulted in $7.2\% \pm 2.5\%$ loading efficiency⁽³³⁾ and scutellarin-loaded BSA nanoparticles possess 64.46% EE and 6.73% DL.⁽³⁴⁾

Fluorescence spectroscopy. The phenomenon of fluorescence quenching can result from various inter- and intramolecular interactions such as energy transfer, conformational changes, complex formation (static quenching), or collisional interaction (dynamic quenching). During static quenching, the quencher forms a stable nonfluorescent complex with the fluorophore, however, during dynamic quenching it collides with the fluorophore and facilitates nonradiative transitions to the ground state.⁽³⁵⁾ Therefore, quenching of the intrinsic fluorescence of the two tryptophan residues (Trp-134 and Trp-212) of BSA can offer information about the changes in molecular microenvironment of these fluorophores, located in domain I and II, respectively. Trp-134 residue is located close to the protein surface in a hydrophilic environment, whereas Trp-212 is within a protein pocket that is hydrophobic (subdomain II A). The Trp-214 in HSA is located similarly to Trp-212 in BSA.^(36–38)

The quenching effect of Api on fluorescence intensity of serum albumins (BSA and HSA) has been studied previously,^(36,39–42) but there are no data related to its behavior in a nanoparticulate system. Studies have shown that the increasing concentration of Api resulted in a decrease in the fluorescence emission intensity of serum albumin solutions. This was mainly attributed to complex formation (static quenching), however, it could be dynamic quenching at higher Api concentrations.⁽⁴²⁾ Nevertheless, all studies concluded that Api most likely binds to the subdomain IIA of Site I side with electrostatic and hydrophobic interactions, through which H-bonds and nonradiative energy transfer can occur. The binding could affect the conformation of Trp microregion, but the secondary structure of serum albumin is not altered.^(36,39,41) However, the pH and ionic concentrations (e.g., NaCl) can affect the fluorescence quenching on the binding parameters of apigenin to BSA.⁽⁴³⁾

Figure 2 demonstrates the fluorescence emission spectra of BSA solution, BSA-NPs, and BSA-Api-NPs. The

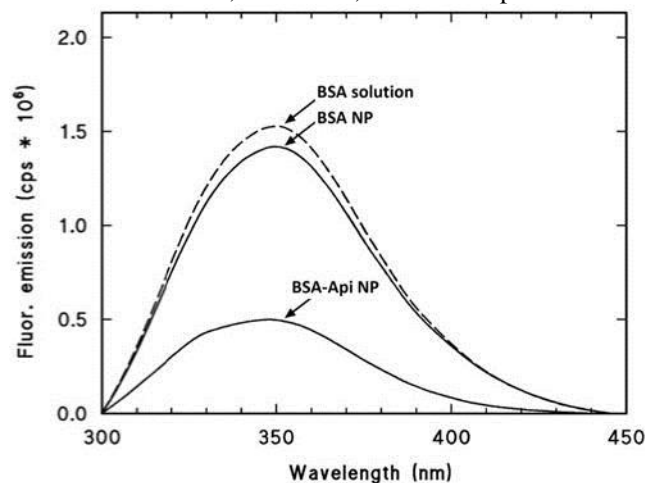


FIG. 2. Fluorescence emission spectra of BSA solution, BSA nanoparticles, and BSA-Api nanoparticles. The excitation wavelength was set to 285 nm. BSA, bovine serum albumin.

fluorescence intensity of BSA-NPs decreased slightly compared to BSA solution with no obvious shift of the maximum position at 350nm. It was probably due to the conformational changes of the protein. The significantly lower emission intensity of BSA-Api-NPs indicates that Api could quench the fluorescence of BSA, which is also reflected on the 3D projections (Fig. 3). All of these findings indicate that Api binds to the Trp region (Trp-212, subdomain II A), but the spectral maximum was not affected, and therefore, hydrophobicity and polarity of the fluorophore residues are not altered. It was concluded that Api can be bound to the Trp region of serum albumin nanoparticles similarly to the solutions.

Characterization of spray-dried BSA-Api-NPs

Determination of residual moisture. Moisture content is mainly influenced by the spray drying conditions. Increased heat energy availability provided by regulating inlet air temperature and aspirator capacity allows more efficient drying, thus resulting in the lower moisture content demonstrated. However, degradation of heat-sensitive materials such as proteins may occur; therefore, inlet air temperature should be kept below 120°C.⁽⁴⁴⁾ The water content is also affected by the type of excipients and the ratio with the nanoparticles.⁽⁴⁵⁾ Moisture content is an important factor that can significantly influence the aerodynamic properties of aerosols. It can change the surface of particles, promote aggregation, and influence the crystallinity of the spray-dried samples.⁽⁴⁴⁾

In this study, the residual water content was determined by using Karl Fisher titration. All formulations had relatively low moisture content, which followed the rank order of L-leucine (4.11% - 0.21%, w/w) < excipient-free (4.55% - 0.49%, w/w) < lactose (5.8% - 0.36%, w/w) containing products. These results demonstrate that the optimized outlet air temperature (around 65 °C) was suitable for serum albumin. The L-leucine containing formulation had the lowest water content due to the low hygroscopic behavior of this amino acid.^(46,47) The low moisture content can potentially improve the flowability and consequently enhance lung deposition due to reduced aggregation as expected. Storage conditions are also important, for example, the spray-dried amorphous lactose particles could transform into crystals easily in humidity above 30%.⁽⁴⁸⁾

Fourier transform infrared spectroscopy. FT-IR analysis allows a quick and efficient identification of the compounds and by their functional groups and bond vibrations. In the spectrum of raw Api, the following characteristic regions were observed: 2710–2580 cm^{-1} O-H bond, 1730–1680 cm^{-1} C=O stretch, and 1450–1380 cm^{-1} C-H bend. A broad peak observed at 3300 cm^{-1} can be attributed to O-H stretching and those bands at 1600–1400 cm^{-1} (C-C stretch in ring) and 900–675 cm^{-1} (C-H “oop”) can be assigned to the aromatic group (Fig. 4A). In the spectrum of BSA protein, the amide I band at 1635 cm^{-1} (mainly C=O stretch) and amide II band at 1530–1500 cm^{-1} (C-N stretching and N-H bend) can be seen. The medium broad peak at 3276 cm^{-1} corresponds to bonded N-H stretch of amide and a smaller band at 1057 cm^{-1}

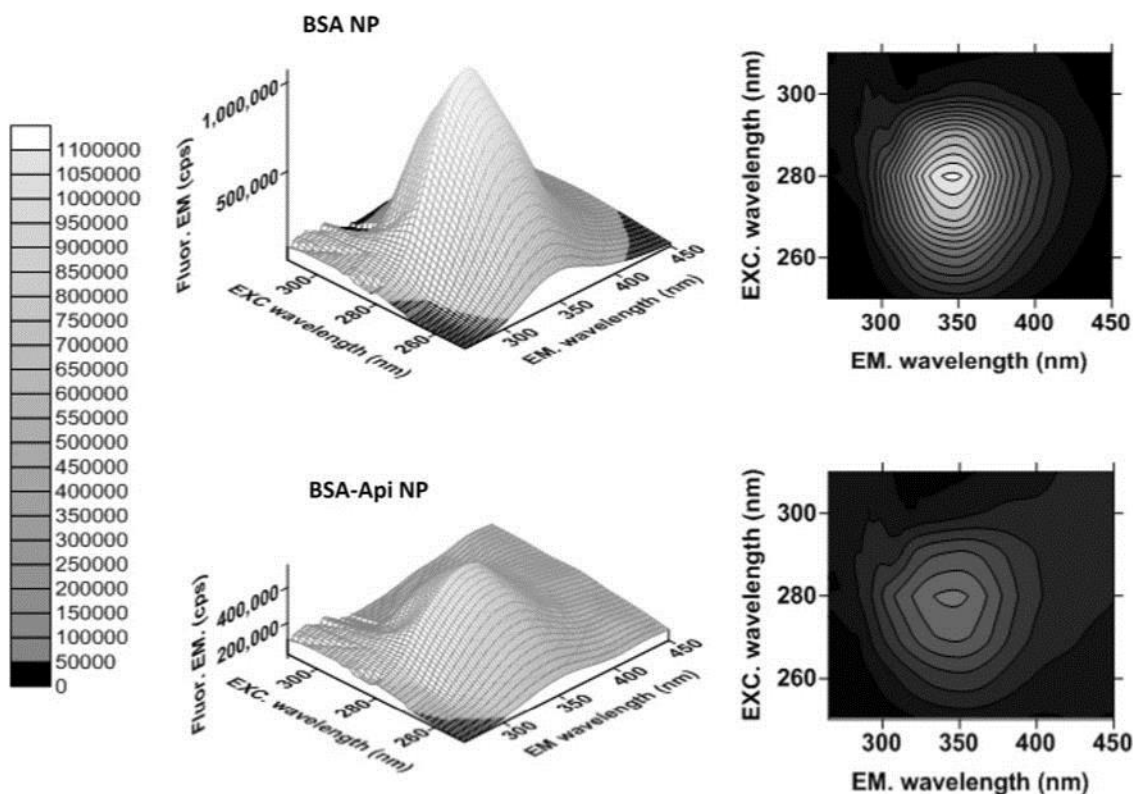


FIG. 3. Three-dimensional fluorescence emission maps and two-dimensional contour maps of empty BSA nanoparticles and BSA-Api nanoparticles. Color scale displays the range of observed fluorescence intensities. EM, emission; EXC, excitation.

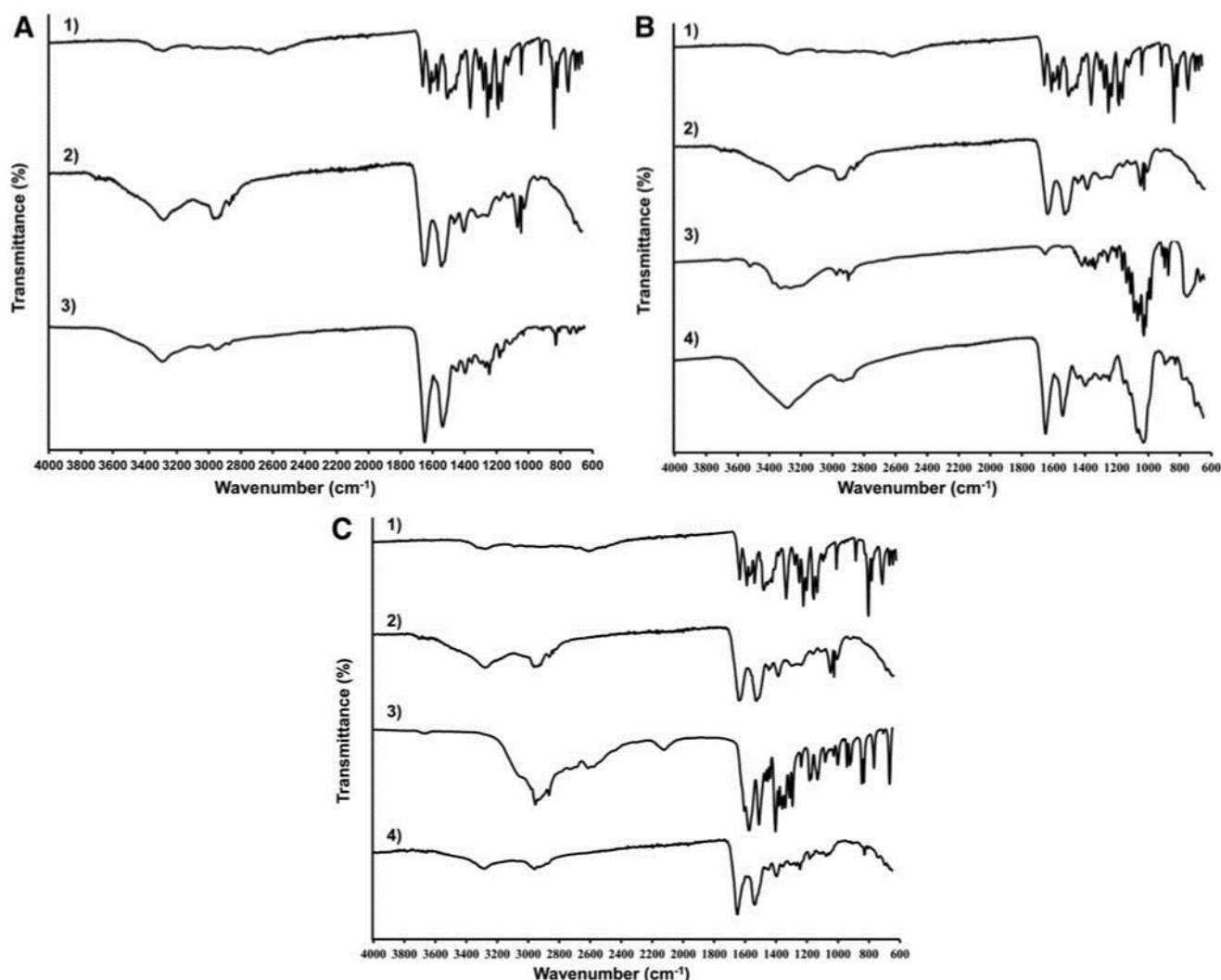


FIG. 4. (A) FT-IR spectra of apigenin (1), BSA (2), and the excipient-free spray-dried BSA-Api nanoparticles (3). (B) FT-IR spectra of apigenin (1), BSA (2), lactose (3), and spray-dried BSA-Api nanoparticles with lactose (4). (C) FT-IR spectra of apigenin (1), BSA (2), L-leucine (3), and spray-dried BSA-Api nanoparticles with L-leucine (4). FT-IR, Fourier transform infrared spectroscopy.

is the C-N stretch of aliphatic amine. In the spectra of the excipient-free formulation, the characteristic amide bands of BSA can be seen and peak at 830 cm⁻¹ indicating the presence of Api (aromatic), which is an indirect confirmation of Api encapsulation on BSA-NPs. Conformational changes can be suggested due to the lack of the peak of aliphatic amine.

The spectra of raw Api, BSA, lactose, and lactose containing product are displayed in Figure 4B. In the spectra of lactose, there is also a broad band around 3300 cm⁻¹ indicating the stretching vibration of hydroxyl group. A weak band at 1654 cm⁻¹ is the bending vibration of the crystalline water and peaks at 1200–1070 cm⁻¹ demonstrating the stretching vibration of C-O-C in the glucose and galactose. The spectrum of amorphous lactose has the less number and defined peaks and therefore it could be distinguished from the crystalline spectrum.⁽⁴⁹⁾ The characteristic broad band at 3300 cm⁻¹ in the spectrum of spray-dried product could originate from the residual water content that is further supported by the Karl Fischer titration data (lactose containing product had the highest water content). Similarly to the spectrum of excipient-free formulation, the amide bands

of BSA and a small peak of Api could be observed. The peaks at 1200–1070cm⁻¹ demonstrate the lactose content and the amorphous state could be assumed.

Functional groups of L-leucine lead to its characteristic spectrum (Fig. 4C). The strong band in the region of 2970–2910 cm⁻¹ can be accounted for the aliphatic C-H stretching. The bonded N-H stretch is present in the region of 2600–2450 cm⁻¹. The NH₂ bending and the C-N skeletal vibration appear in the regions of 1595–1550 cm⁻¹ and 1250–1020 cm⁻¹.⁽⁵⁰⁾ The presence of BSA characteristic peaks on the spray-dried formulation could be mainly observed with a small peak of Api, but the major characteristic peaks of L-leucine are obscured.

X-ray powder diffraction. XRPD is considered to be the most accurate method to study crystalline structure.⁽⁵¹⁾ The combined XRPD diffractograms of Api and spray-dried

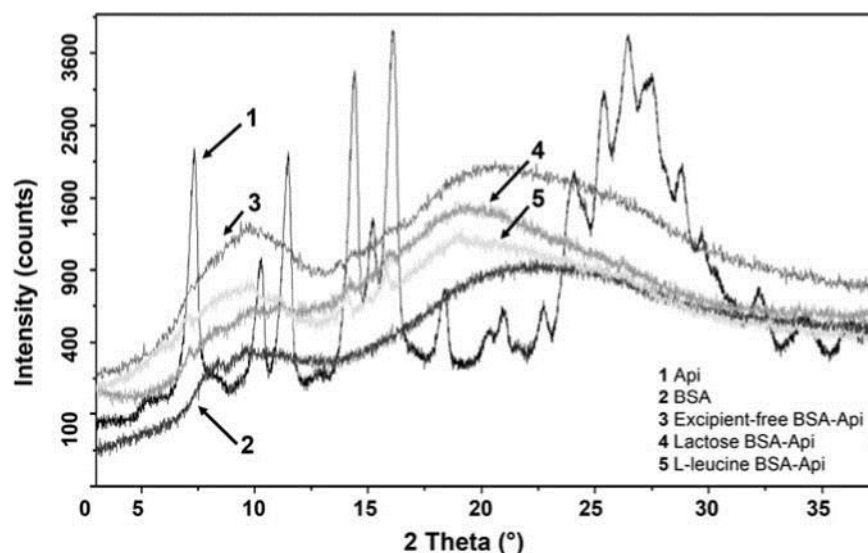


FIG. 5. X-ray powder diffraction pattern of raw apigenin and the formulations.

formulations are presented in Figure 5. The characteristic narrow diffraction peaks of Api are due to the crystalline state of the commercially available material. In comparison, broad diffuse peaks could be observed in the diffractograms of the spray-dried formulations suggesting the amorphous state of BSA-Api-NPs. The observed XRD patterns of spray-dried L-leucine and lactose were consistent with literature.^(48,52,53)

DSC analysis. The DSC curves of raw Api, excipients, physical mixtures, and spray-dried formulations were studied to examine crystallinity. As seen in Figure 6, there is only one sharp endothermic peak at 360°C indicating the melting point of raw Api; no impurities were observed. Drug-free albumin exhibited two broad peaks with onset values of 220°C and 310°C. The evaporation of residual water occurred at 50–120°C. The melting point of Api on the thermograms of raw material and physical mixtures corresponds to the crystalline habitus.

In the thermograms of physical mixtures in Figure 6B, the endothermic peak at 140°C indicating the crystalline lactose⁽⁵⁴⁾ and the sublimation of L-leucine crystals occurred at 200°C–230°C (Fig. 6C).⁽⁵⁵⁾ However, in each spray-dried formulation, the absence of endotherms confirms the loss of crystallinity. No peak could be observed around 360°C indicating that Api is in an amorphous state due to the spray drying process, which is in agreement with the XRPD diffractograms. The amorphous form generated may result in higher solubility of the powders and dissolution of apigenin in lung fluids.

Aerosol particle size analysis and redispersibility in water. Dry powder formulations of BSA-Api-NPs were prepared with the aim of studying the influence of excipients on the particle size and aerodynamic behavior. The deposition of aerosols is significantly affected by particle size, which should be small enough to pass through the upper airways and large enough to avoid exhalation.⁽⁵⁶⁾ Gravitational sedimentation is the main driving force for deposition of a nanoparticulate system in the lung due to the formation of aggregates in the micrometer size range. Particle geometry and surface properties also play a significant role in reaching the bronchioles.^(22,32) It is well known that particles can be

deposited efficiently deeper in the lung if their aerodynamic diameter is in the range of 1–5 µm and only those with 1–3 µm can reach the respiratory zone.⁽⁵⁷⁾ Particles, larger than 5 µm, tend to deposit in the oropharynx and the mucociliary clearance plays a role in clearing the particles toward the pharynx. However, very small particles, less than 1 µm are usually exhaled because of the low inertia.^(58,59)

Mucociliary clearance is part of the natural defense mechanism of the lung as well as the phagocytosis of macrophages in the alveolar region. The aerosol particle size was determined by Sympatec HELOS laser diffractometer (Table 1). The excipient-free and lactose containing products have similar sizes, while spray drying with L-leucine produced the smallest particles ($D_{50} = 2.473 \mu\text{m}$). In all cases, the particle size could ensure the highest probability of delivery of apigenin into the respiratory zone.

Following the redispersion of spray powder formulations in distilled water, the size of the particles was preserved in the nanometer size range: without excipient ($358.9 \pm 5.3 \text{ nm}$, PDI: 0.315 ± 0.013), lactose ($366.1 \pm 4.8 \text{ nm}$, PDI: 0.382 ± 0.014), and L-leucine ($343.7 \pm 2.9 \text{ nm}$, PDI: 0.316 ± 0.011) containing products. Spray drying has no significant effect on the average size of the particles, suggesting the deposition of apigenin containing nanoparticles in the lung fluid. Moreover, the excipients did not affect adversely the particle size.

Solubility and drug release studies of BSA-Api formulations. The solubility of apigenin in nanoparticles was investigated in PBS buffer and mSLF (Fig. 7A). The results showed that the solubility was slightly increased in mSLF media (82%–98% within 5 minutes), however, it was high in PBS buffer as well (79%–95% within 5 minutes). These data indicated that the solubility of apigenin could be highly enhanced by BSA nanoparticles in aqueous medium. Nevertheless, the dispersibility enhancers could play a role in the solubility. In case of excipient-free formulation, 91% of the encapsulated apigenin was dissolved in mSLF within 5 minutes. Formulation prepared with lactose increased the

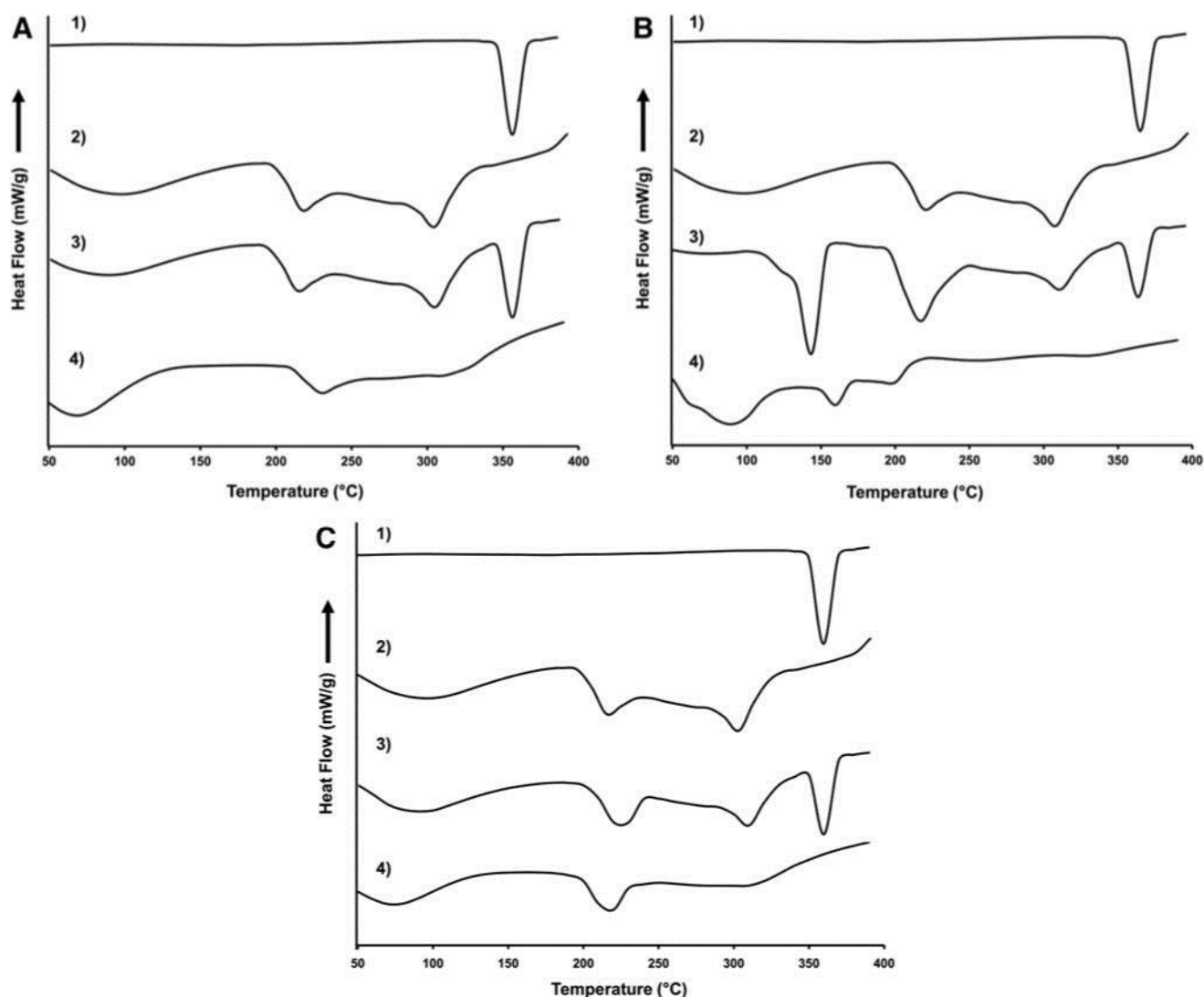


FIG. 6. (A) DSC thermograms of apigenin (1), BSA (2), physical mixture (3), and excipient-free spray-dried BSA-API nanoparticles (4). (B) DSC spectra of apigenin (1), BSA (2), physical mixture (3), and spray-dried BSA-API nanoparticles with lactose (4). (C) DSC spectra of apigenin (1), BSA (2), physical mixture (3), and spray-dried BSA-API nanoparticles with L-leucine (4). DSC, differential scanning calorimetry.

solubility rate up to 98%, however, it was slower (82%) when using L-leucine and completed within 2 hours. These results could be attributed to the solubility of the excipients themselves; lactose has very good water solubility, but L-leucine possesses a low solubility in water.⁽⁵⁵⁾

TABLE 1. AEROSOL PARTICLE SIZES OF SPRAY-DRIED NANOPARTICLES WITH SYMPATEC HELOS LASER DIFFRACTOMETER IN 1M

| | <i>Excipient free</i> | <i>Lactose</i> | <i>L-leucine</i> |
|-----------|-----------------------|----------------|------------------|
| ED (%) | 91.862±2.735 | 93.950±1.046 | 95.183±0.667 |
| FPF (%) | 65.617±3.422 | 58.463±6.031 | 66.090±2.777 |
| MMAD (1m) | 3.210±0.069 | 3.130±0.001 | 2.123±0.098 |
| GSD (1m) | 2.823±0.113 | 2.270±0.212 | 1.887±0.063 |
| RD (%) | 99.1±5.012 | 94.7±4.091 | 96.3 ±2.161 |

ED, emitted dose; FPF, fine particle fraction; GSD, geometric standard deviation; MMAD, mass median aerodynamic diameter; RD, recovered dose.

The apigenin release from the spray-dried BSA-API-NPs was investigated with Franz cell apparatus. It is a well-

known device for the dissolution of semisolid dosage forms and approved by the USP. However, there is no standardized method for inhaled powders, Franz cell could be one of the alternative choices due to simulating the diffusion-controlled air-liquid interface of the lung. On the contrary, it has some limitations such as small air bubbles under the contact area of membrane to dissolution medium, wide range of SD, or recovery usually around maximum 90%.⁽⁶⁰⁾ Based on the solubility measurements, mSLF was applied.

The cumulative dissolution curves of the prepared formulations are shown in Figure 7B. As expected, the dissolution was affected by the cospray-dried excipients. Lactose containing product resulted the fastest and highest apigenin release due to the excellent water solubility. This enhancement of the dissolution is supported by previously published data.⁽⁶¹⁾ In contrast, the dissolution rate was decreased when L-leucine was applied. The coating layer of L-leucine slowed

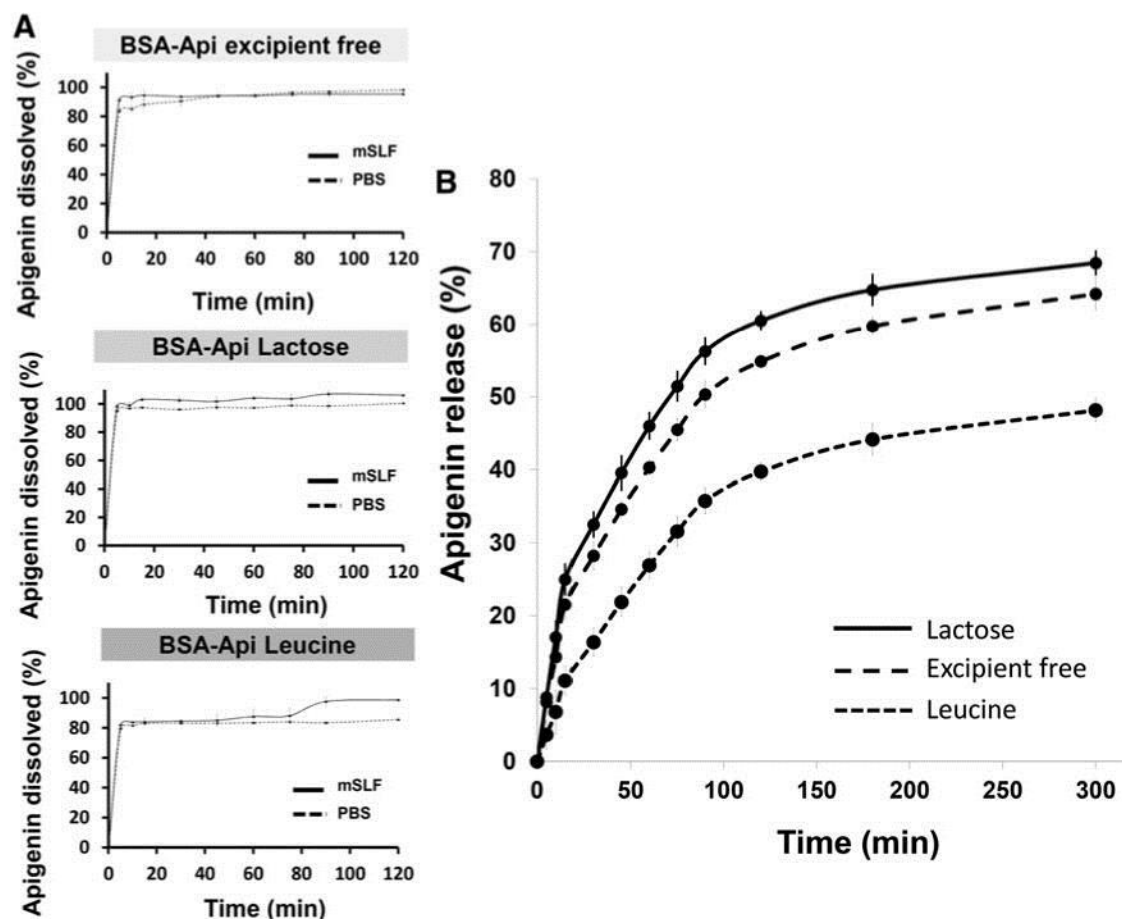


FIG. 7. (A) Solubility of spray-dried BSA-Api formulations in PBS buffer and mSLF). (B) Dissolution of apigenin from the formulations as a function of time in mSLF. mSLF, modified simulated lung fluid.

down the dissolution of apigenin, which could be well observed in the dissolution curve. The low water solubility of L-leucine is able to hinder the dissolution of the drug, which was published previously.⁽⁵⁵⁾ These results suggest that the excipients play an important role in the solubility and the dissolution as well.

Aerosol delivery of BSA-Api formulations. Particles can be taken up by alveolar macrophages, which influence the therapeutic outcome. Those nanoparticles that are soluble and above 200 nm are able to escape from the macrophages and therefore exhibit sustained therapeutic effect.⁽⁶²⁾ The lung deposition and therefore the efficacy of the inhaled therapeutics are governed by their aerosol properties.⁽⁵⁶⁾ Manufacturing respirable nanoparticles could be produced by aggregation in the favorable size range or their incorporation into microparticles (1–5 μm).⁽²⁶⁾

Lactose monohydrate is a well-known, traditional carrier for improving the performance of inhaled products; however, it is influenced by physicochemical properties and interaction with the active ingredient.^(63,64) It is the only FDA-approved carrier and has also been shown to be a potential excipient for protein encapsulation.^(27,64) Recently, novel materials such as specific amino acids have been developed for pulmonary formulations⁽²⁶⁾ and L-leucine is one of the most effective dispersibility enhancer among them.⁽⁴⁷⁾ Previous studies proved that 5% (w/w) L-leucine improved the aerosol performance of raw naringin⁽⁶⁵⁾ and

inclusion up to 15% (w/w) L-leucine resulted in higher ED and FPF of powder formulation of gentamicin.⁽⁴⁶⁾

In this study, *in vitro* aerosol properties of three different dry powder formulations were evaluated using the NGI, which is regarded as an optimal instrument for analysis of aerodynamic behavior of aerosol formulations for pulmonary drug delivery⁽⁶⁶⁾ according to the European and US Pharmacopeias. The obtained data and deposition pattern are presented in Table 2 and in Figure 8. It can be seen that more than 90% of apigenin could be recovered from the NGI, which is in the acceptable pharmacopeia range (75–125%). The ED ranged between 91% and 96% indicating good flowability and high dispersibility of the powders. L-leucine containing formulation had the highest ED as it could improve significantly the flowability of the powders.^(47,53)

TABLE 2. AERODYNAMIC CHARACTERISTIC OF SPRAY-DRIED NANOPARTICLES

| | <i>Excipient free</i> | <i>Lactose</i> | <i>L-leucine</i> |
|-----------------|-----------------------|----------------|------------------|
| D ₁₀ | 1.033 ± 0.032 | 1.020 ± 0.070 | 0.843 ± 0.680 |
| D ₅₀ | 3.030 ± 0.092 | 3.107 ± 0.102 | 2.473 ± 0.300 |
| D ₉₀ | 7.110 ± 0.306 | 7.117 ± 0.337 | 5.287 ± 0.670 |

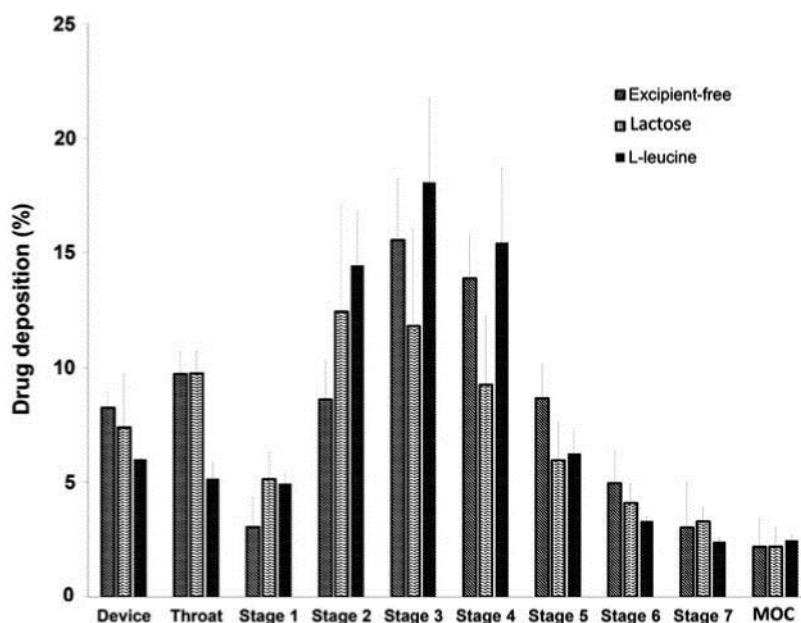


FIG. 8. Next-generation impactor deposition pattern of the spray-dried BSA-Api formulations.

Figure 8 shows the amount of Api deposited on the throat device and Stages 1–7 expressed as a percentage of the total amount of recovered powder. All formulations exhibited increased deposition in Stage 2–4, indicating enhanced drug delivery to the alveolar regions. As expected, improved aerosol performance and deposition (Stage 3 and 4) could be observed when L-leucine was used as an excipient. The FPF is one of the key parameters in aerosol delivery and should be as high as possible.⁽⁶⁷⁾ In this study, the FPF values ranged between 58% and 66%, suggesting that the particles could be delivered into the peripheral regions. Spray drying of nanoparticles in the presence of L-leucine resulted in a higher FPF value (66%) due to improved surface properties and morphology of the particles.⁽⁶⁴⁾

In general, MMAD values $<5 \mu\text{m}$ are for pulmonary lung delivery and between 2 and 3 μm are optimal for deep lung deposition.⁽⁵⁶⁾ In each case, the calculated MMAD data were in agreement with the physical diameter size of the particles measured by laser diffractometer. The data obtained ($<5 \mu\text{m}$) support good dispersibility of the particles into the lower airways and the deep lung. Therefore, local delivery to the alveoli could be assured by both excipient-free and lactose formulations generated (MMAD 3.2 and 3.1 μm). Moreover, formulation with L-leucine (MMAD 2.1 μm) would be more optimal for deep lung deposition. The size distribution of an aerosol is described best by GSD.⁽⁶⁸⁾ Based on the GSD data obtained, the L-leucine containing formulation had the narrowest size distribution (1.8 μm) but that of the others was also in the acceptable range ($<3 \mu\text{m}$).

The overall values demonstrate that the particles of each dry powder nanoparticle formulation are in the favorable aerodynamic size range, possess good dispersibility properties and particle deposition. Therefore, BSA-NPs are an attractive delivery system for pulmonary drug delivery. We demonstrated that L-leucine improved better the aerosolization properties of BSA-Api-NPs than lactose monohydrate. Therefore, it can be concluded that the use of excipients influences the aerosol performance of nanoparticles.

Particle morphology. SEM analysis was conducted to investigate the morphology of the powders (Fig. 9A, B). It is well known that the morphology of the particles is strongly affected by the solubility of the components and the nature of the excipients.^(46,47) The commercially available Api was a crystalline powder featuring needle-shaped crystals. The excipient-free spray-dried nanoparticles exhibited a spherical shape and smooth or wrinkled surface. Particles of lactose containing product had raisin-like surface and some of the particles were larger in accordance with the laser diffraction particle size analysis.

Powders prepared with L-leucine comprised small and collapsed particles with a strongly corrugated surface. The low aqueous solubility of L-leucine leading to a shell on the surface of the droplet that interferes with the diffusion of water; therefore, corrugated particles could form. This outcome was consistent with previous observations.^(46,53,69) Corrugated surface improves the dispersibility of the dry powder formulations and enhances respirability due to reduced interparticulate cohesion (Van der Waals forces), which is beneficial for particles intended for inhalation.⁽⁷⁰⁾

Antioxidant activity

Owing to its reproducibility and comparability, the DPPH assay is an established method for investigating the antioxidant properties of natural compounds. Due to the H-donating ability of the antioxidants, a stable reduced DPPH-H molecule can form. The reaction can be seen visually and the detection can be carried out using UV-Vis spectrophotometer.^(71,72) Previous studies confirmed that Api is able to scavenge the DPPH free radical even in nanoscale delivery formulation.^(73,74) In general, the scavenging activity is influenced by concentration and structural features such as hydrogen donating ability, position, and the degree of

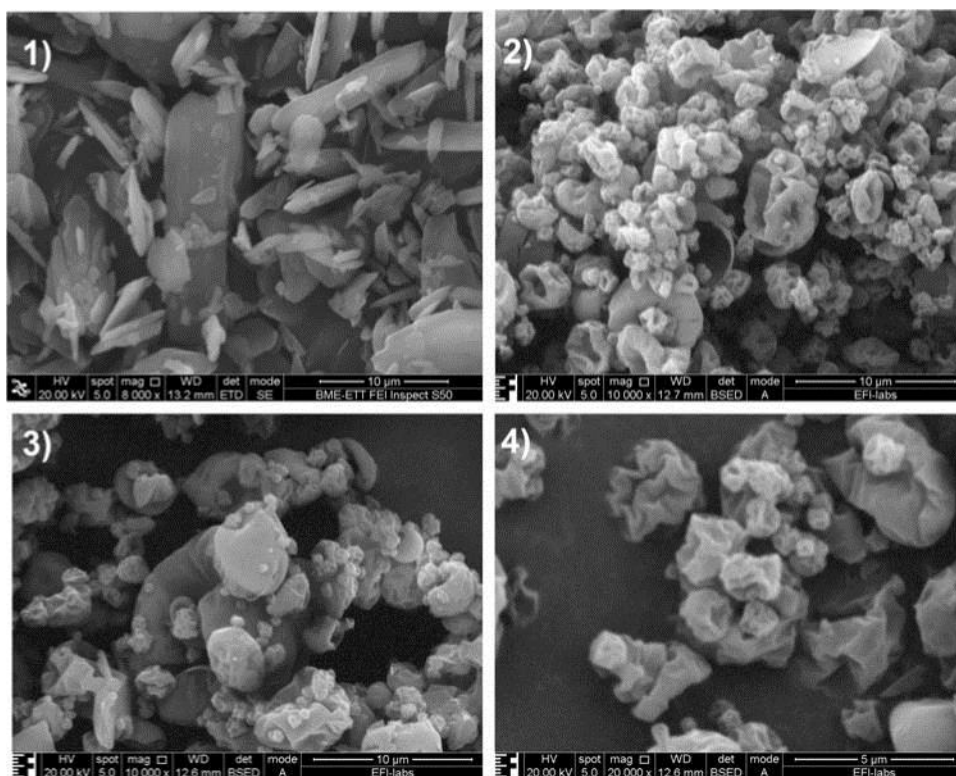


FIG. 9. Scanning electron microscopy images of raw apigenin (1), excipient-free spray-dried BSA-Apigenin nanoparticles (2), spray-dried BSA-Apigenin nanoparticles with lactose (3), and spray-dried BSA-Apigenin nanoparticles with L-leucine (4) 20,000 magnification.

hydroxylation.^(75,76) To calculate the exact concentration of remaining DPPH in the samples, a calibration curve was plotted with $R^2 = 0.9999$. The time required to reach the steady state was estimated to be 120 minutes, and the slow reaction kinetic of Api has been reported.⁽⁷³⁾ The discolor-

ation of the deep purple DPPH free radical indicates the antioxidant properties of free and encapsulated Api.

The inhibition of free radicals by the prepared spray-dried formulations was compared to the empty BSA-NPs, methanolic Api solution, and "empty" nanoparticles (Fig. 10).

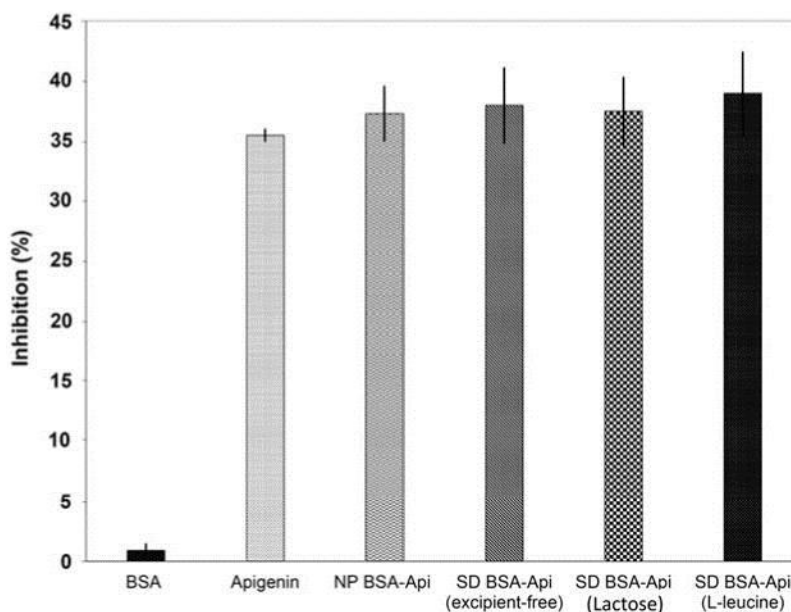


FIG. 10. Radical scavenging activity of Apigenin solution, empty BSA nanoparticles, BSA-Apigenin nanoparticles (NP), and spray-dried nanoparticles (SD) with excipients. The antioxidant activity is expressed as the inhibition of DPPH free radical in percent. DPPH, 2,2-diphenyl-1-picrylhydrazyl.

It can be seen that the free and encapsulated Api has similar scavenging activity, moreover, spray drying did not result in the loss of scavenging activity. It has been reported that serum albumin is a physiological circulating antioxidant in the body,⁽⁷⁷⁾ which is confirmed by the inhibition capacity of the empty BSA-NPs observed. Similar results were reported when encapsulating rutin and kaempferol⁽⁷⁸⁾ or quercetin,⁽¹⁷⁾ where the antioxidant activity of the flavonoids are retained by BSA. It can be concluded that the antioxidant activity of Api is preserved, moreover, slightly enhanced by the BSA.

Conclusion

In this study, novel apigenin containing albumin nanoparticles were prepared for inhalation against lung injury caused by oxidative stress. Apigenin was recently classified as a BCS II drug with prominent antioxidant and anti-inflammatory properties in the lung. The obtained results confirmed that incorporation of apigenin into the biocompatible albumin nanoparticles resulted in high encapsulation efficiency, and therefore, it could be an attractive tool for delivery. Moreover, the spray-dried nanoparticles possess good ability to redisperse in aqueous media and size of the particles was preserved in the nanometer size range.

The influence of dispersibility enhancers on the physicochemical properties and *in vitro* pulmonary deposition was investigated and compared to the excipient-free formulation. The obtained *in vitro* pulmonary depositions proved that the developed BSA-NP dry powders are potentially able to carry apigenin deep in the lung, reaching the respiratory zone. The use of novel excipient amino acid L-leucine resulted in enhanced aerodynamic properties over the traditional lactose monohydrate, indicating that the nature of the excipients and morphology of the particles play a significant role in the formulation of nanoparticles for pulmonary delivery. In addition, the solubility and dissolution characteristics of apigenin from nanoparticles were determined in mSLF dissolution media, the cospray-dried excipients played an important role.

The dissolution rate was increased by the water soluble lactose and decreased by L-leucine, which has low water solubility. Therefore, the use of excipients should be taken into consideration, and may not be required in case of albumin nanoparticles. We further confirmed that the antioxidant activity is retained; thus, the potential of albumin nanoparticles as an effective pulmonary delivery system for flavonoids such as apigenin.

Acknowledgment

The authors gratefully acknowledge Robert Kovács for providing the SEM pictures at Budapest University of Technology and Economics.

Author Disclosure Statement

No competing financial interests exist.

References

1. Chow C-W, Herrera Abreu MT, Suzuki T, and Downey GP: Oxidative stress and acute lung injury. *Am J Respir Cell Mol Biol*. 2003;29:427–431.
2. Chen XW, Serag ES, Sneed KB, and Zhou SF: Herbal bioactivation, molecular targets and the toxicity relevance. *Chem Biol Interact*. 2011;192:161–176.
3. Patel D, Shukla S, and Gupta S: Apigenin and cancer chemoprevention: Progress, potential and promise (review). *Int J Oncol*. 2007;30:233–245.
4. Kim SJ, Jeong HJ, Moon PD, Lee KM, Lee HB, Jung HJ, Jung SK, Rhee HK, Yang DC, Hong SH, and Kim HM: Anti-inflammatory activity of gumiganghwaltang through the inhibition of nuclear factor-kappa B activation in peritoneal macrophages. *Biol Pharm Bull*. 2005;28:233–237.
5. Kowalski J, Samojedny A, Paul M, Pietsz G, and Wilczok T: Effect of apigenin, kaempferol and resveratrol on the expression of interleukin-1beta and tumor necrosis factor-alpha genes in J774.2 macrophages. *Pharmacol Rep*. 2005;57:390–394.
6. Lee J-H, Zhou H, Cho S, Kim Y, Lee Y, and Jeong C: Anti-inflammatory mechanisms of apigenin: Inhibition of cyclooxygenase-2 expression, adhesion of monocytes to human umbilical vein endothelial cells, and expression of cellular adhesion molecules. *Arch Pharm Res*. 2007;30:1318–1327.
7. Chen L, and Zhao WEI: Apigenin protects against bleomycin-induced lung fibrosis in rats. *Exp Ther Med*. 2016; 11:230–234.
8. Luan RL, Meng XX, and Jiang W: Protective effects of apigenin against paraquat-induced acute lung injury in mice. *Inflammation*. 2016;39:752–758.
9. Basios N, Lampropoulos P, Papalois A, Lambropoulou M, Pitiakoudis MK, Kotini A, Simopoulos C, and Tsaroucha AK: Apigenin attenuates inflammation in experimentally induced acute pancreatitis-associated lung injury. *J Invest Surg*. 2015;2:1–7.
10. Patil R, Babu RL, Naveen Kumar M, Kiran Kumar KM, Hegde S, Ramesh G, and Chidananda Sharma S: Apigenin inhibits PMA-induced expression of pro-inflammatory cytokines and AP-1 factors in A549 cells. *Mol Cell Biochem*. 2015;403:95–106.
11. Wang J, Liu Y-T, Xiao L, Zhu L, Wang Q, and Yan T: Anti-inflammatory effects of apigenin in lipopolysaccharide-induced inflammatory in acute lung injury by suppressing COX-2 and NF-kB Pathway. *Inflammation*. 2014;37:2085–2090.
12. Zhang J, Liu D, Huang Y, Gao Y, and Qian S: Biopharmaceutics classification and intestinal absorption study of apigenin. *Int J Pharm*. 2012;436:311–317.
13. Ajazuddin, and Saraf S: Applications of novel drug delivery system for herbal formulations. *Fitoterapia*. 2010;81:680–689.
14. Elzoghby AO, Samy WM, and Elgindy NA: Albumin-based nanoparticles as potential controlled release drug delivery systems. *J Control Release*. 2012;157:168–182.
15. Hu Y-J, Liu Y, Sun T-Q, Bai A-M, Lu J-Q, and Pi Z-B: Binding of anti-inflammatory drug cromolyn sodium to bovine serum albumin. *Int J Biol Macromol*. 2006;39:280–285.
16. Fasano M, Curry S, Terreno E, Galliano M, Fanali G, Narciso P, Notari S, and Ascenzi P: The extraordinary ligand binding properties of human serum albumin. *IUBMB Life*. 2005;57:787–796.
17. Fang R, Hao R, Wu X, Li Q, Leng X, and Jing H: Bovine serum albumin nanoparticle promotes the stability of quercetin in simulated intestinal fluid. *J Agr Food Chem*. 2011;59:6292–6298.

18. He X, Xiang N, Zhang J, Zhou J, Fu Y, Gong T, and Zhang Z: Encapsulation of teniposide into albumin nanoparticles with greatly lowered toxicity and enhanced antitumor activity. *Int J Pharm.* 2015;487:250–259.
19. Muralidharan P, Malapit M, Mallory E, Hayes D, Jr., and Mansour HM: Inhalable nanoparticulate powders for respiratory delivery. *Nanomedicine.* 2015;11:1189–1199.
20. Malcolmson RJ, and Embleton JK: Dry powder formulations for pulmonary delivery. *Pharm Sci Technol Today.* 1998;1:394–398.
21. Stegemann S, Kopp S, Borchard G, Shah VP, Senel S, Dubey R, Urbanetz N, Cittero M, Schoubben A, Hippchen C, Cade D, Fuglsang A, Morais J, Borgström L, Farshi F, Seyfang KH, Hermann R, van de Putte A, Klebovich I, and Hincal A: Developing and advancing dry powder inhalation towards enhanced therapeutics. *Eur J Pharm Sci.* 2013;48:181–194.
22. Yang W, Peters JI, and Williams RO, 3rd: Inhaled nanoparticles—A current review. *Int J Pharm.* 2008;356:239–247.
23. Geiser M: Update on macrophage clearance of inhaled micro- and nanoparticles. *J Aerosol Med Pulm Drug Deliv.* 2010;23:207–217.
24. Woods A, Patel A, Spina D, Riffo-Vasquez Y, Babin-Morgan A, de Rosales RT, Sunassee K, Clark S, Collins H, Bruce K, Dailey LA, and Forbes B: In vivo biocompatibility, clearance, and biodistribution of albumin vehicles for pulmonary drug delivery. *J Control Release.* 2015;210:1–9.
25. Swarbrick J: *Encyclopedia of Pharmaceutical Technology.* Informa Healthcare, London; pp. 671–1434, 2007.
26. Mansour HM, Rhee YS, and Wu X: Nanomedicine in pulmonary delivery. *Int J Nanomedicine.* 2009;4:299–319.
27. Shoyele SA, and Cawthorne S: Particle engineering techniques for inhaled biopharmaceuticals. *Adv Drug Deliv Rev.* 2006;58:1009–1029.
28. Sung JC, Pulliam BL, and Edwards DA: Nanoparticles for drug delivery to the lungs. *Trends Biotechnol.* 2007;25:563–570.
29. Desai NP, Tao C, Yang A, Louie L, Yao Z, Soon-Shiong P, and Magdassi S: Protein stabilized pharmacologically active agents, methods for the preparation thereof and methods for the use thereof. Google Patents, 2004. US6749868 B1.
30. Son YJ, and McConville JT: Development of a standardized dissolution test method for inhaled pharmaceutical formulations. *Int J Pharm.* 2009;382:15–22.
31. Hatano T, Kagawa H, Yasuhara T, and Okuda T: Two new flavonoids and other constituents in licorice root—their relative astringency and radical scavenging effects. *Chem Pharm Bull.* 1988;36:2090–2097.
32. Paranjpe M, and Muller-Goymann CC: Nanoparticle-mediated pulmonary drug delivery: A review. *Int J Mol Sci.* 2014;15:5852–5873.
33. Kim TH, Jiang HH, Youn YS, Park CW, Tak KK, Lee S, Kim H, Jon S, Chen X, and Lee KC: Preparation and characterization of water-soluble albumin-bound curcumin nanoparticles with improved antitumor activity. *Int J Pharm.* 2011;403:285–291.
34. Wei Y, Li L, Xi Y, Qian S, Gao Y, and Zhang J: Sustained release and enhanced bioavailability of injectable scutellarin-loaded bovine serum albumin nanoparticles. *Int J Pharm.* 2014;476:142–148.
35. Valeur B: *Molecular Fluorescence Principles and Applications.* Wiley-VCH, Weinheim, Germany; pp. 73–124, 2002.
36. Yuan J-L, lv Z, Liu Z-G, Hu Z, and Zou G-L: Study on interaction between apigenin and human serum albumin by spectroscopy and molecular modeling. *J Photochem Photobiol A.* 2007;191:104–113.
37. Naveenraj S, and Anandan S: Binding of serum albumins with bioactive substances—Nanoparticles to drugs. *J Photochem Photobiol C.* 2013;14:53–71.
38. Tayeh N, Rungassamy T, and Albani JR: Fluorescence spectral resolution of tryptophan residues in bovine and human serum albumins. *J Pharm Biomed Anal.* 2009;50:107–116.
39. Zhao X-N, Liu Y, Niu L-Y, and Zhao C-P: Spectroscopic studies on the interaction of bovine serum albumin with surfactants and apigenin. *Spectrochim Acta A Mol Biomol Spectrosc.* 2012;94:357–364.
40. Lin C-Z, Hu M, Wu A-Z, and Zhu C-C: Investigation on the differences of four flavonoids with similar structure binding to human serum albumin. *J Pharm Anal.* 2014;4:392–398.
41. Cao H, Liu Q, Shi J, Xiao J, and Xu M: Comparing the affinities of flavonoid isomers with protein by fluorescence spectroscopy. *Anal Lett.* 2008;41:521–532.
42. Shang Y, and Li H: Studies of the interaction between apigenin and bovine serum albumin by spectroscopic methods. *Russ J Gen Chem.* 2010;80:1710–1717.
43. Tang L, Jia W, and Zhang D: The effects of experimental conditions of fluorescence quenching on the binding parameters of apigenin to bovine serum albumin by response surface methods. *Luminescence.* 2014;29:344–351.
44. Stahl K, Claesson M, Lilliehorn P, Linden H, and Backstrom K: The effect of process variables on the degradation and physical properties of spray dried insulin intended for inhalation. *Int J Pharm.* 2002;233:227–237.
45. Jensen DM, Cun D, Maltesen MJ, Frokjaer S, Nielsen HM, and Foged C: Spray drying of siRNA-containing PLGA nanoparticles intended for inhalation. *J Control Release.* 2010;142:138–145.
46. Aquino RP, Protta L, Auriemma G, Santoro A, Mencherini T, Colombo G, and Russo P: Dry powder inhalers of gentamicin and leucine: Formulation parameters, aerosol performance and in vitro toxicity on CuF11 cells. *Int J Pharm.* 2012;426:100–107.
47. Yang X-F, Xu Y, Qu D-S, and Li H-Y: The influence of amino acids on aztreonam spray-dried powders for inhalation. *Asian J Pharm Sci.* 2015;10:541–548.
48. Wu L, Miao X, Shan Z, Huang Y, Li L, Pan X, Yao Q, Li G, and Wu C: Studies on the spray dried lactose as carrier for dry powder inhalation. *Asian J Pharm Sci.* 2014;9:336–341.
49. Listiohadi Y, Hourigan J, Sleigh R, and Steele R: Thermal analysis of amorphous lactose and α -lactose monohydrate. *Dairy Sci Technol.* 2009;89:43–67.
50. Némec I, and Mic'ka Z: FTIR and FT Raman study of L-leucine addition compound with nitric acid. *J Mol Struct.* 1999;482–483:23–28.
51. Newman AW, and Byrn SR: Solid-state analysis of the active pharmaceutical ingredient in drug products. *Drug Discov Today.* 2003;8:898–905.
52. Sou T, Kaminskas LM, Nguyen T-H, Carlberg R, McIntosh MP, and Morton DAV: The effect of amino acid excipients on morphology and solid-state properties of multi-component spray-dried formulations for pulmonary delivery of biomacromolecules. *Eur J Pharm Biopharm.* 2013;83:234–243.
53. Mangal S, Meiser F, Tan G, Gengenbach T, Denman J, Rowles MR, Larson I, and Morton DAV: Relationship between surface concentration of l-leucine and bulk powder properties in spray dried formulations. *Eur J Pharm Biopharm.* 2015;94:160–169.

54. Gombás A, Szabó-Révész P, Kata M, Regdon G, Jr., and Erős I: Quantitative determination of crystallinity of α -lactose monohydrate by DSC. *J Therm Anal Calorim.* 2002; 68:503–510.
55. Raula J, Seppälä J, Malm J, Karppinen M, and Kauppinen EI: Structure and dissolution of l-leucine-coated salbutamol sulphate aerosol particles. *AAPS PharmSciTech.* 2012;13:707–712.
56. Yang MY, Chan JGY, and Chan H-K: Pulmonary drug delivery by powder aerosols. *J Control Release.* 2014;193: 228–240.
57. Chow AL, Tong HY, Chattopadhyay P, and Shekunov B: Particle engineering for pulmonary drug delivery. *Pharm Res.* 2007;24:411–437.
58. Liang Z, Ni R, Zhou J, and Mao S: Recent advances in controlled pulmonary drug delivery. *Drug Discov Today.* 2015; 20:380–389.
59. Heyder J, Gebhart J, Rudolf G, Schiller CF, and Stahlhofen W: Deposition of particles in the human respiratory tract in the size range 0.005–15 μ m. *J Aerosol Sci.* 1986;17:811–825.
60. May S, Jensen B, Wolkenhauer M, Schneider M, and Lehr CM: Dissolution techniques for in vitro testing of dry powders for inhalation. *Pharm Res.* 2012;29:2157–2166.
61. Knieke C, Azad MA, To D, Bilgili E, and Davé RN: Sub-100 micron fast dissolving nanocomposite drug powders. *Powder Technol.* 2015;271:49–60.
62. Patel B, Gupta N, and Ahsan F: Particle engineering to enhance or lessen particle uptake by alveolar macrophages and to influence the therapeutic outcome. *Eur J Pharm Biopharm.* 2015;89:163–174.
63. Kou X, Chan LW, Steckel H, and Heng PWS: Physicochemical aspects of lactose for inhalation. *Adv Drug Deliv Rev.* 2012;64:220–232.
64. Pilcer G, Wauthoz N, and Amighi K: Lactose characteristics and the generation of the aerosol. *Adv Drug Deliv Rev.* 2012;64:233–256.
65. Prota L, Santoro A, Bifulco M, Aquino RP, Mencherini T, and Russo P: Leucine enhances aerosol performance of Naringin dry powder and its activity on cystic fibrosis airway epithelial cells. *Int J Pharm.* 2011;412:8–19.
66. Taki M, Marriott C, Zeng X-M, and Martin GP: Aerodynamic deposition of combination dry powder inhaler formulations in vitro: A comparison of three impactors. *Int J Pharm.* 2010;388:40–51.
67. Davis SS: Delivery of peptide and non-peptide drugs through the respiratory tract. *Pharm Sci Technol Today.* 1999;2:450–456.
68. Musante CJ, Schroeter JD, Rosati JA, Crowder TM, Hickey AJ, and Martonen TB: Factors affecting the deposition of inhaled porous drug particles. *J Pharm Sci.* 2002;91:1590–1600.
69. Lechuga-Ballesteros D, Charan C, Stults CL, Stevenson CL, Miller DP, Vehring R, Tep V, and Kuo MC: Trileucine improves aerosol performance and stability of spray-dried powders for inhalation. *J Pharm Sci.* 2008;97:287–302.
70. Chew NY, and Chan HK: The role of particle properties in pharmaceutical powder inhalation formulations. *J Aerosol Med.* 2002;15:325–330.
71. Brand-Williams W, Cuvelier ME, and Berset C: Use of a free radical method to evaluate antioxidant activity. *LWT Food Sci Technol.* 1995;28:25–30.
72. Villaño D, Fernández-Pachón MS, Moyá ML, Troncoso AM, and García-Parrilla MC: Radical scavenging ability of polyphenolic compounds towards DPPH free radical. *Talanta.* 2007;71:230–235.
73. Al Shaal L, Shegokar R, and Muller RH: Production and characterization of antioxidant apigenin nanocrystals as a novel UV skin protective formulation. *Int J Pharm.* 2011; 420:133–140.
74. Papay ZE, Antal I. Study on the antioxidant activity during the formulation of biological active ingredient. *Eur Sci J.* 2014; Special Edition 3:252–257.
75. Yang J, Guo J, and Yuan J: In vitro antioxidant properties of rutin. *LWT Food Sci Technol.* 2008;41:1060–1066.
76. Natella F, Nardini M, Di Felice M, and Scaccini C: Benzoic and cinnamic acid derivatives as antioxidants: structure-activity relation. *J Agr Food Chem.* 1999;47:1453–1459.
77. Roche M, Rondeau P, Singh NR, Tarnus E, and Bourdon E: The antioxidant properties of serum albumin. *FEBS Lett.* 2008;582:1783–1787.
78. Fang R, Jing H, Chai Z, Zhao G, Stoll S, Ren F, Liu F, and Leng X: Study of the physicochemical properties of the BSA: Flavonoid nanoparticle. *Eur Food Res Technol.* 2011; 233:275–283.

Address correspondence to:
István Antal, PhD
Department of Pharmaceutics
Semmelweis University
H. Gyögyes E. Street 7-9
Budapest H-1092
Hungary

[E-mail: antal.istvan@pharma.semmelweis-univ.hu](mailto:antal.istvan@pharma.semmelweis-univ.hu)